

# Accepted Manuscript

Solubility profiles, hydration and desolvation of curcumin complexed with  $\gamma$ -cyclodextrin and hydroxypropyl- $\gamma$ -cyclodextrin

Sergey Shityakov, Ramin Ekhteiari Salmas, Serdar Durdagi, Norbert Roewer, Carola Förster, Jens Broscheit



PII: S0022-2860(16)31318-7

DOI: [10.1016/j.molstruc.2016.12.028](https://doi.org/10.1016/j.molstruc.2016.12.028)

Reference: MOLSTR 23226

To appear in: *Journal of Molecular Structure*

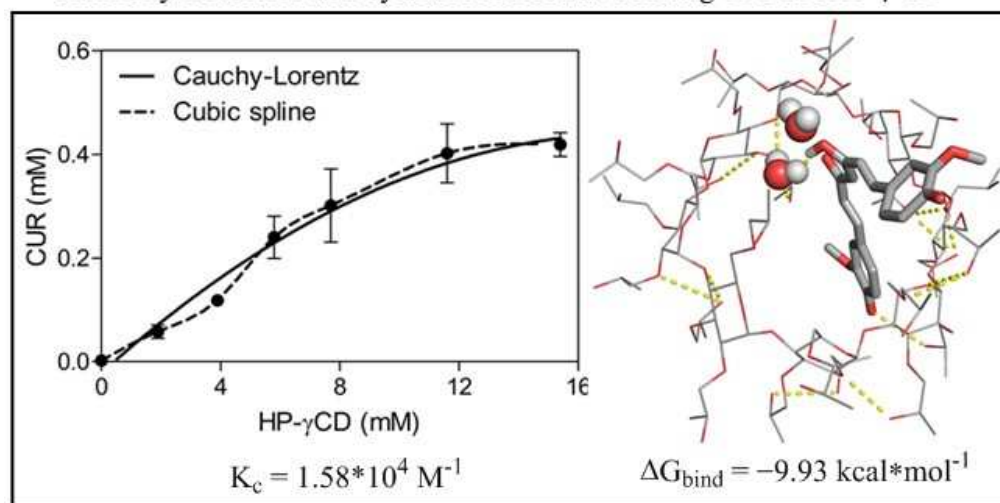
Received Date: 22 July 2016

Revised Date: 6 December 2016

Accepted Date: 9 December 2016

Please cite this article as: S. Shityakov, R.E. Salmas, S. Durdagi, N. Roewer, C. Förster, J. Broscheit, Solubility profiles, hydration and desolvation of curcumin complexed with  $\gamma$ -cyclodextrin and hydroxypropyl- $\gamma$ -cyclodextrin, *Journal of Molecular Structure* (2017), doi: 10.1016/j.molstruc.2016.12.028.

This is a PDF file of an unedited manuscript that has been accepted for publication. As a service to our customers we are providing this early version of the manuscript. The manuscript will undergo copyediting, typesetting, and review of the resulting proof before it is published in its final form. Please note that during the production process errors may be discovered which could affect the content, and all legal disclaimers that apply to the journal pertain.

solubility isotherms and hydrated molecular docking of CUR/HP- $\gamma$ -CD

# Solubility profiles, hydration and desolvation of curcumin complexed with $\gamma$ -cyclodextrin and hydroxypropyl- $\gamma$ -cyclodextrin

Sergey Shityakov<sup>1,\*</sup>, Ramin Ekhteiari Salmas<sup>3</sup>, Serdar Durdagi<sup>3</sup>, Norbert Roewer<sup>1,2</sup>,  
Carola Förster<sup>1</sup>, and Jens Broscheit<sup>1,2</sup>

<sup>1</sup>Department of Anesthesia and Critical Care, University of Würzburg, 97080 Würzburg, Germany

<sup>2</sup>Sapiotec Ltd., 97078 Würzburg, Germany

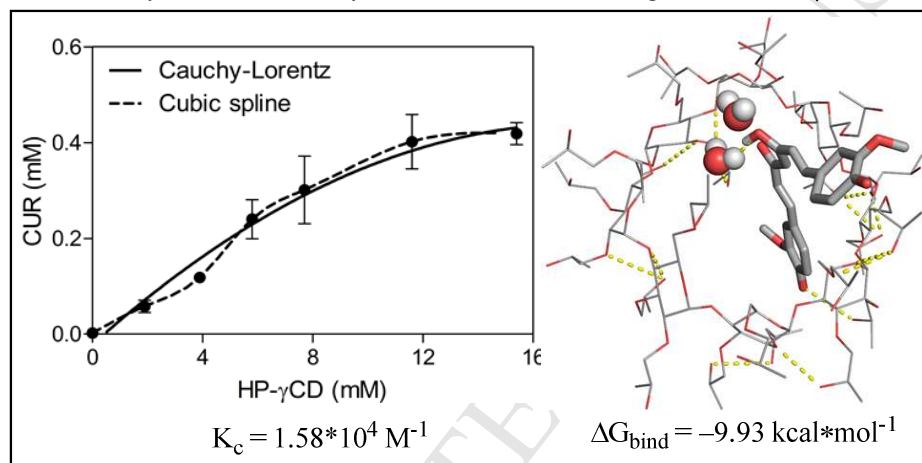
<sup>3</sup>Department of Biophysics, School of Medicine, Bahcesehir University, Istanbul, Turkey

Author to whom correspondence should be addressed; E-Mail: Shityakov\_s@ukw.de

Tel: +49-931-2013-0016; Fax: +49-931-2013-0019.

## Graphical Abstract:

solubility isotherms and hydrated molecular docking of CUR/HP- $\gamma$ -CD



**Abstract:** In this study, we investigated curcumin (CUR) solubility profiles and hydration/desolvation effects of this substance formulated with  $\gamma$ -cyclodextrin ( $\gamma$ -CD) and hydroxypropyl- $\gamma$ -cyclodextrin (HP- $\gamma$ -CD) excipients. The CUR/HP- $\gamma$ -CD complex was found to be more stable in solution with the highest apparent stability constant for CUR/HP- $\gamma$ -CD ( $K_c = 1.58 \times 10^4 \text{ M}^{-1}$ ) as the more soluble form in distilled water. The *in silico* calculations, including molecular docking, Monte Carlo (MC), and molecular dynamics (MD) simulations, indicated that water molecules play an important role in host-guest complexation mediating the CUR binding to cyclodextrins via hydrogen bond formations. The CUR hydration/desolvation effects contributed to the complex formation by elevating the CUR binding affinity to both CDs. The CUR/HP- $\gamma$ -CD complex after the CUR hydration was determined with a minimal Gibbs free energy of binding ( $\Delta G_{\text{bind}} = -9.93 \text{ kcal} \cdot \text{mol}^{-1}$ ) due to the major hydrophobic (vdW) forces. Overall, the results of this study can aid a development of cyclodextrin-based drug

34 delivery vectors, signifying the importance of water molecules during the formulation  
35 processes.

36

37 **Keywords:** curcumin, cyclodextrins, complex stability, hydrated molecular docking,  
38 hydrogen bonds, Monte Carlo, molecular dynamics simulations, free energy calculations

39

## 40 **1. Introduction**

41 Curcumin (CUR) is a natural chemical produced by some plants of the ginger family, and it is  
42 used as a dietary herbal supplement or a food coloring agent (Volate et al., 2005; Baumann et  
43 al., 2009). This substance has also been found to possess antiviral and anticancer properties,  
44 which were intensively characterized over the last few decades (Nagabhushan and Bhide,  
45 1992; Prasad and Tyagi, 2015). The CUR compound is essentially insoluble at physiological  
46 pH and, since it is very unstable, it undergoes a rapid hydrolytic degradation (Tonnesen et al.,  
47 2002). Various attempts have been made to produce water-soluble and more stable CUR by  
48 formulating it with different excipients, including hydrophilic cyclodextrins (CDs) to  
49 minimize its hydrolysis and high decomposition rate (Yadav et al., 2009; Marcolino et al.,  
50 2011).

51 CDs have a wide range of biomedical applications in fields such as pharmacy, chemistry,  
52 biotechnology, and medicine. They are oligosaccharides produced by bacteria from starch via  
53 its enzymatic degradation and typically exist as pristine hexameric  $\alpha$ -, heptameric  $\beta$ - and  
54 octameric  $\gamma$ -CD forms and their derivatives (Zidovetzki and Levitan, 2007). CDs have a  
55 hydrophilic outer surface, and a less polar but more lipophilic (amphiphilic) central cavity  
56 leading to a CD inclusion complexation with different drug-like substances through the  
57 electrostatic, van der Waals (vdW), hydrophobic, charge-transfer, and H-bonding interactions.  
58 The CD-drug complex formation usually contributes to a retardation of the degradation rate  
59 during solvation process (Tonnesen et al., 2002). This complexation process mainly depends  
60 on the interaction of the guest molecule with CDs and the difference in the interactions of  
61 bound water and water with the bulk solvent. Therefore, studies on molecular recognition and  
62 binding require careful consideration of solvent effects.

63 The solvated drug molecules interact with waters before they bind to CDs with a subsequent  
64 release of water molecules to the bulk waters in aqueous solution. This so-called “desolvation  
65 process” is usually unfavorable during the change in Gibbs free energy of binding ( $\Delta G_{\text{bind}}$ )  
66 and described as a “desolvation” penalty (Baldwin, 2010). However, some water molecules

67 are not displaced, and they might mediate the CD-drug complexation via altering binding site  
68 topography followed by the increase in overall binding affinity.

69 To tackle this issue, different quantitative and qualitative approaches have been established  
70 and applied to assess the energy contribution implied by the presence or displacement of  
71 water molecules, such as the hydrated ligand molecular docking (Forli and Olson, 2012). In  
72 particular, the AutoDock method was recently revised to evaluate the solvation and  
73 desolvation phenomena via including explicit displaceable waters during molecular docking  
74 procedure to improve overall docking precision and scoring function without excessive  
75 computational needs (Forli and Olson, 2012). On the other hand, to the best of our knowledge,  
76 there is no report on the hydration effect of CUR complexed with cyclodextrins so far.  
77 Therefore, in the present study, we have investigated the solubility profiles and the CUR  
78 hydration/desolvation process contribution to the CUR complexation with  $\gamma$ -CD and  
79 hydroxypropyl- $\gamma$ -CD (HP- $\gamma$ -CD) using combined experimental and computational techniques.

80

## 81 **2. Materials and Methods**

### 82 *2.1. Materials*

83 CUR was purchased from Sigma-Aldrich GmbH (Steinheim am Albuch, Germany). The  
84 CUR/ $\gamma$ -CD and CUR/HP- $\gamma$ -CD complexes as pure forms (98% purity) were prepared as per  
85 the following protocols: 45 g of  $\gamma$ -CD and 5 g of CUR were weighed and suspended in 25 ml  
86 distilled water with a mortar and a pestle. Similarly, 1 g of HP- $\gamma$ -CD and 44 mg of CUR were  
87 weighed and suspended in 1.5 ml of 96% ethanol and were homogenized as above. After  
88 complete homogenization, the suspension was dried *in vacuo* under ambient conditions for  
89 three days. Finally, the dried complexes were pulverized in the mortar.

90

### 91 *2.2. Quantification of curcumin*

92 The CUR concentrations were determined by UV/Vis spectrophotometry using an Agilent  
93 8453 spectroscopy system (Agilent Technologies, Budapest, Hungary). The samples were  
94 diluted with a 50 vol% ethanol-water mixture to yield an absorbance recordable at the 430 nm  
95 range. All CUR measurements were performed without any interference from CDs presented  
96 in the complex.

97

### 98 *2.3. Solubility studies and determination of stability constants*

99 The solubility method was carried out according to the Higuchi & Connors method (Higuchi  
100 and Connors, 1965). Solubilities were measured by adding an excess amount of curcumin to  
101 distilled water containing different amounts of various kinds of cyclodextrins. The suspension  
102 formed was equilibrated under continuous agitation for 24 h at  $25 \pm 3.0$  °C and then filtered  
103 through a 0.45  $\mu\text{m}$  nominal pore size PVDF filter to yield a clear curcumin solution. The  
104 apparent stability constant ( $K_c$ ) for a CUR-CD complexes was obtained from the slope of the  
105 phase-solubility diagram according to the following equation:

$$K_c = \frac{\text{slope}}{S_0(1 - \text{slope})} \quad (1)$$

106 where  $S_0$  is the saturation concentration of CUR in the solvent without cyclodextrin. The data  
107 are represented as means  $\pm$  S.D. of three independent experiments.

108

#### 109 2.4. Molecular docking and semi-empirical calculations

110 The 3D coordinates of the curcumin structure were retrieved from the PubChem database  
111 (Figure 1[A]). Since no 3D structure for HP- $\gamma$ -CD was available, the molecule was  
112 constructed from the  $\gamma$ -CD (PDB ID: 1P2G) crystal structure (Pinotsis et al., 2003) with the  
113 PyMol v.1.2 software (Figure 1 [B]). Prior to molecular docking and semi-empirical  
114 calculations, the all-simulated structures were minimized with the GTKDynamo v.1.8.1  
115 software (Bachega et al., 2013) using the conjugate gradient method with 200 maximum  
116 iterations and a threshold tolerance gradient of 0.1 Å. The host and guest structure  
117 preparations for molecular docking included the Gasteiger partial charge assignment  
118 (Gasteiger et al., 1980) and rotatable bonds definition. Rigid-flexible standard and hydrated  
119 molecular docking were applied to the center of the cyclodextrin structure. AutoDock  
120 v.4.2.5.1 (Goodsell et al., 1996; Forli et al., 2015) integrated into the PyMol AutoDock/Vina  
121 plugin (Seeliger and Groot, 2010) was used in the study. The grid spacing of 0.375 Å, with a  
122 dimension size of 60 Å from x, y, and z, was used to create the grid maps. In order to increase  
123 a conformational sampling of the drug, a number of genetic algorithm dockings (ga\_run) were  
124 set to 100. Docking output results were represented by the approximation function as the  
125 estimated Gibbs free energy of binding ( $\Delta G_{\text{bind}}$ ). The calculated octanol/water partition  
126 (ClogP) coefficient for curcumin using the weighted algorithm with electrolyte concentration  
127 of 0.1 mol/dm<sup>3</sup> and its aqueous solubility (ClogS) were determined by the Marwin Sketch  
128 v.14.7.14.0 tool. The single-point calculations for all simulated structures using the Austin

129 Model 1 (AM1) method (Dewar et al., 1985; Rocha et al., 2006) were performed using  
130 GTKDynamo v.1.8.1 software (Bachega et al., 2013).

131

### 132 *2.5. Atomistic molecular dynamics (MD) simulations*

133 The docking poses of CUR produced by AutoDock v.4.2.5.1 (Goodsell et al., 1996; Forli et  
134 al., 2015) were used as an initial structure suitable for MD simulations. All classical MD  
135 simulations were performed using a GPU-accelerated version of Desmond 2015.4 code  
136 (Bowers et al., 2006). The OPLS 2005 force field (Banks et al., 2005) was used to calculate the  
137 interactions between atoms. The long-range electrostatic interaction calculations were set up  
138 by using the particle-mesh Ewald (PME) method (Essmann et al., 1995). The short-range van  
139 der Waals (vdW) and Coulomb interactions were defined by a cut-off radius of 9.0 Å. A Nose-  
140 Hoover thermostat (Hoover et al., 1985) and Martyna-Tobias-Klein method (Martyna et al.,  
141 1994) were used to maintain the system at the body temperature of 310 K and the pressure of  
142 1.01325 bars. A time step of 2.0 fs was used during the MD simulations. The systems were  
143 minimized using 2000 iterations, and a convergence threshold of 1 kcal\*mol<sup>-1</sup>\*Å<sup>-1</sup>. To perform  
144 the structural relaxation, all the systems were equilibrated using default algorithms  
145 implemented in the Desmond software. Finally, 100 ns atomistic MD trajectories were  
146 produced for each of the analyzed systems.

147

### 148 *2.6. Monte Carlo simulations*

149 All Monte Carlo (MC) simulations implemented in ROSETTA code (Meiler et al., 2006) were  
150 employed in order to generate different systematic conformers for the standard and hydrated  
151 variants of CUR bound to  $\gamma$ -CD and HP- $\gamma$ -CD. The trajectory frames as obtained by the MC  
152 protocol were subjected to conformational clustering to be used further for the Molecular  
153 Mechanics with Generalized Born and Surface Area Solvation (MM-GBSA) energy analysis  
154 (Gohlke et al., 2004).

155

### 156 *2.7. MM-GBSA calculations*

157 The MM-GBSA method (Gohlke et al., 2004) was applied to estimate the free energies of  
158 binding ( $\Delta G_{\text{MM-GBSA}}$ ) for the CUR-CD complexes. The Prime module in the Schrödinger  
159 package (Schrödinger Release 2014-2: Prime, version 3.6) was used to calculate the  $\Delta G_{\text{MM-}}$   
160  $\text{GBSA}$  values. The VSGB 2.0 solvation model (Li et al., 2011) was used to simulate the implicit  
161 solvation for the analyzed systems. The  $\Delta G_{\text{MM-GBSA}}$  values were determined by subtracting the

162 total individual free energies of cyclodextrin ( $\Delta G_{CD}$ ) and CUR ( $\Delta G_{CUR}$ ) from the complex  
 163 free energy ( $\Delta G_{\text{complex}}$ ) as depicted according to the following equation:

$$\Delta G_{MM-GBSA} = \Delta G_{\text{complex}} - (\Delta G_{CD} + \Delta G_{CUR}) \quad (2)$$

164 or re-written as a sum of the energetic terms:

$$\Delta G_{MM-GBSA} = \Delta G_{\text{Coul}} + \Delta G_{\text{cov}} + \Delta G_{H\text{-bond}} + \Delta G_{\text{lipo}} + \Delta G_{\text{solv}} + \Delta G_{\text{vdW}} \quad (3)$$

165 where  $\Delta G_{\text{Coul}}$ ,  $\Delta G_{\text{cov}}$ ,  $G_{H\text{-bond}}$ ,  $\Delta G_{\text{lipo}}$ ,  $\Delta G_{\text{solv}}$  and  $\Delta G_{\text{vdW}}$  are Columb, covalent, hydrogen-bond,  
 166 lipophilic, GB electrostatic solvation and vdW energies, respectively.

167

### 168 3. Results and Discussion

169 Molecular modelling techniques, such as molecular docking, have been proven useful in  
 170 predicting the binding modes and interaction profiles of drug-like molecules complexed with  
 171 different target structures including CDs (Ansari et al., 2012; Kar et al., 2013; Ahsan et al.,  
 172 2015; Shityakov et al., 2016). In the standard and hydrated molecular docking experiments,  
 173 the enol form of CUR, that is more energetically stable in the solid phase (Manolova et al.,  
 174 2014) because of intramolecular hydrogen bonding, was chosen as the ligand. While  $\gamma$ -CD  
 175 and HP- $\gamma$ -CD were selected to be the excipient macromolecules. Taking into account the  
 176 flexibility of CUR and CD, different conformational variants for the complexes are possible.  
 177 By adding the ligand molecule to the CDs, 100 docking conformation instances for each  
 178 CUR/CD pair were generated.

179 The conformation of a guest compound can depend strongly on the presence of solvent  
 180 molecules participating in the binding and mediation of the interactions between different  
 181 ligand substitutes and the receptor (Forli and Olson, 2012). For this reason, studies of  
 182 molecular complexation involving cyclodextrins require careful consideration of the solvent  
 183 effects. Nonetheless, the formation of the CUR/CD complex takes place primarily in the  
 184 aqueous phase, and is followed by the drying step under ambient conditions. Even then, the  
 185 complex still contains approximately 6.9% residual water, established by the Karl Fischer  
 186 titration method.

187 In an aqueous environment, the  $\gamma$ -CD cavity with the largest volume ( $427 \text{ \AA}^3$ ) in comparison  
 188 to other CDs ( $174 \text{ \AA}^3$  for  $\alpha$ -CD and  $262 \text{ \AA}^3$  for  $\beta$ -CD) is occupied with water molecules; and  
 189 most or all of these water molecules are excluded from the cavity upon binding with a guest  
 190 compound. This mildly lipophilic cavity, which contains about 9 weakly-held and easily  
 191 displaced water molecules with higher enthalpy than the bulk waters (Tabushi et al., 1978;

192 Tanhuanpää et al., 2001). Also, because of the H-bond bivalency of this binding site, a water  
193 molecule can “invert” a receptor's hydrogen bond acceptor region into a donor (Forli and  
194 Olson, 2012). The cavity is further stabilized by intramolecular H-bonds between the adjacent  
195 primary and secondary hydroxyl groups in  $\gamma$ -CD and hydroxypropyl groups in HP- $\gamma$ -CD.

196 Water molecules were attached to CUR before docking by hydrating all polar groups capable  
197 of hydrogen bond interactions. This is important information in *de novo* or early stages of  
198 drug design, to optimize the ligands to best fit the binding site. As already mentioned in the  
199 literature,  $\gamma$ -CD, and its derivative can be topologically described as torus-shaped molecules  
200 with the larger and the smaller entries, where the hydroxyl groups are exposed to the solvent  
201 (Munro et al., 2004). Previous studies (Szejtly, 1998; Uekama et al., 1998; Ma et al., 2000;  
202 Zhao et al., 2002) have verified that the ligand molecule is usually inserted into CDs via the  
203 larger outer rim opening (0.85 nm) instead of the smaller (0.75 nm) one. In fact, our docking  
204 simulations demonstrate a similar scenario where CUR was inserted into the binding cavity of  
205 the amphiphilic CDs from the larger interface in both the standard and hydrated variants. The  
206 water molecules remained in the vicinity of the outer rim, and some of them were deeply  
207 submerged into the cyclodextrin binding cavity, interacting with the enolic hydroxyl group of  
208 CUR via H-bonds (Figure 2 and 3).

209 Based on the above observation of the CUR docking poses, only the complex structure with  
210 predicted the lowest  $\Delta G_{\text{bind}}$  value in the binding region was considered as the top-docking  
211 result. The results are listed in Table 1 for standard and hydrated molecular dockings. CUR  
212 was found to bind strongly to CDs exceeding the binder/non-binder energy threshold (non-  
213 binders  $< -6.0 \text{ kcal}\cdot\text{mol}^{-1} <$  binders), where this threshold for various drug-like molecules in  
214 other AutoDock experiments has been determined (Shityakov et al., 2012; Shityakov et al.,  
215 2014). The CUR hydration improves its binding affinity to both cyclodextrins, this was  
216 confirmed by a minimal predicted Gibbs free energy of binding ( $\Delta G_{\text{bind}}$ ) values. The CUR  
217 hydration/desolvation effects contributed to the complex formation by elevating the CUR  
218 binding affinity to both CDs. The CUR/HP- $\gamma$ -CD complex after the CUR hydration was  
219 determined with a minimal Gibbs free energy of binding ( $\Delta G_{\text{bind}} = -9.93 \text{ kcal}\cdot\text{mol}^{-1}$ ) and  $K_d$   
220 of  $0.05 \mu\text{M}$ . The thermodynamic equilibrium constants ( $K_d$ ) for all of the docking poses were  
221 calculated from the  $\Delta G_{\text{bind}}$  values as follows:  $K_d = \exp([\Delta G_{\text{bind}}*1000]/[R*T])$ , where R (gas  
222 constant) is  $1.98 \text{ cal}\cdot(\text{mol}\cdot\text{K})^{-1}$  and T (room temperature) is 298.15 Kelvin (Shityakov *et al.*,  
223 2012).

224 The increase in CUR binding affinity to CDs after hydration might be explained by the higher  
225 number of intermolecular H-bonds formed between the host and the guest: 4 for CUR/ $\gamma$ -CD  
226 and 2 for CUR/HP- $\gamma$ -CD without ligand hydration (Figure 2 [A] and 3 [A]); and 8 for CUR/ $\gamma$ -  
227 CD and 4 for CUR/HP- $\gamma$ -CD with ligand hydration (Figure 2 [B] and 3 [B]). Thus, the CUR  
228 hydrated docking to CDs illustrates the capabilities of the new hydration method to predict the  
229 position of weakly bound water molecules; and we ranked them in accordance with  
230 experimental findings, improving the docking accuracy.

231 The minimal predicted  $\Delta G_{\text{bind}}$  and  $K_d$  values indicated that very lipophilic CUR ( $\log P = 3.28$ )  
232 compound (Pawar et al., 2012) with very low calculated water solubility ( $0.01 - 0.06 \text{ mg} \cdot \text{mL}^{-1}$ )  
233 appeared to be the strongest binder to HP- $\gamma$ -CD in both variants of molecular docking. As a  
234 result of the higher hydrophobicity potential ( $\text{ClogP} = -5.30$ ) defined for this modified  
235 cyclodextrin than for its parental pristine form ( $\text{ClogP} = -14.17$ ).

236 Following this, the top-docked poses of CUR were analyzed for whether the pose was still the  
237 likely bound pose and there are 99 other possible host-guest configurations. Since, there are  
238 several commonly occurring docked poses formed during the clustering with the root-mean-  
239 square-deviation (RMSD) cut-off value of  $2.0 \text{ \AA}$ , the most popular pose was present multiple  
240 times for the standard and hydrated docking simulations. Additionally, when the guest  
241 interacts with water before it binds to the host, then those water molecules must be displaced  
242 to be further released into the bulk of the waters molecules in the solution (Furuki et al.,  
243 1993). The change in  $\Delta G_{\text{bind}}$  in this process is often unfavorable and considered to be the  
244 “desolvation” penalty (Furuki et al., 1993). The determination of water to be displaced or  
245 bridged is the balance between its energetic contribution to ligand-receptor binding and the  
246 ability to stabilize a ligand pose through its displacement (Forli and Olson, 2012). Following  
247 this rule, during the hydrated complexation of CUR with the  $\gamma$ -CD and HP- $\gamma$ -CD molecules  
248 most of the water molecules were displaced because of high water free energy ( $\Delta G_{\text{wat}} = -0.2$   
249  $\text{kcal} \cdot \text{mol}^{-1}$ ) and only few were strongly ( $\Delta G_{\text{wat}} = -0.62 \text{ kcal} \cdot \text{mol}^{-1}$ ) or weakly ( $\Delta G_{\text{wat}} = -0.36$   
250  $\text{kcal} \cdot \text{mol}^{-1}$ ) attached via H-bonds to the inclusion complex (Table 2). Clearly, the CUR  
251 inclusion in the CD cavity cannot lead to the displacement of all water molecules presented in  
252 it. The more closely a guest can be fitted in the CD binding site, the greater will be the  
253 number of water molecules released into the bulk. Thus, the combination of these two effects,  
254 such as CUR inclusion and water displacement, impacts the equilibrium formation constants  
255 for CD formulated drugs in solution.

256 Quantitation of CUR was also determined from the solubility isotherms of the CUR/ $\gamma$ -CD and  
 257 CUR/HP- $\gamma$ -CD complexes in a distilled water. The solubility diagrams for all complexes were  
 258 non-linear Cauchy–Lorentz distribution for CUR/ $\gamma$ -CD and showed second-order polynomial  
 259 (quadratic) curve fitting for CUR/HP- $\gamma$ -CD (Figure 4 [A, B]). The CUR concentration in  
 260 CUR/HP- $\gamma$ -CD was about 60-fold greater than that of  $\gamma$ -CD complex due to improved  
 261 aqueous solubility. The CUR/HP- $\gamma$ -CD solution was supersaturated when the concentration of  
 262 HP- $\gamma$ -CD was higher than 11.6 mM. The CUR/ $\gamma$ -CD precipitate formation was started at 1.9  
 263 mM of  $\gamma$ -CD disturbing the CUR release probably by binding to its free fraction. The plateau  
 264 section of the curve suggested that the precipitation of the complex was finally attained. An  
 265 estimate of  $K_c$  constant was calculated using the analytical detection limit as highest possible  
 266  $S_0$  value ( $S_0 = 2.37 \mu\text{M}$ ) showing the increase in apparent stability for CUR/HP- $\gamma$ -CD ( $K_c =$   
 267  $1.58 \cdot 10^4 \text{ M}^{-1}$ ) in contrast with the CUR/ $\gamma$ -CD complex ( $K_c = 1.02 \cdot 10^3 \text{ M}^{-1}$ ). Observations  
 268 from previous complexation studies on curcuminoids also suggested that the bulky moieties  
 269 of the two phenyl groups of CUR fit better to the bigger  $\gamma$ -CD than  $\beta$ -CD cavity, where the  $K_c$   
 270 values of CUR in HP- $\beta$ -CD and HP- $\gamma$ -CD was reported to be more than  $5.0 \cdot 10^4 \text{ M}^{-1}$  and  
 271  $16 \cdot 10^4 \text{ M}^{-1}$ , respectively (Tonnesen et al., 2002).

272 To compare our experimental and theoretical results, we calculated the reference binding ratio  
 273 ( $BR_{ref}$ ) to determine the complexation strength, which is based on the relative content of CUR  
 274 in the  $\gamma$ -CD ( $C_{\gamma\text{-CD}}$ ) or in HP- $\gamma$ -CD ( $C_{HP\text{-}\gamma\text{-CD}}$ ) complex, molecular weight of the complex  
 275 constituents and degree of substitution ( $n$ ) for HP- $\gamma$ -CD using the following equation:

$$BR_{ref} = \frac{C_{HP\text{-}\gamma\text{-CD}} (MW_{CUR} + MW_{HP\text{-}\gamma\text{-CD}} + n \cdot MW_{res})}{C_{\gamma\text{-CD}} (MW_{HP\text{-}\gamma\text{-CD}} + MW_{HP\text{-}\gamma\text{-CD}})} \quad (4)$$

276 where  $MW_{CUR}$ ,  $MW_{CD}$ , and  $MW_{res}$  are the molecular weights of curcumin,  $\gamma$ -CD, HP- $\gamma$ -CD and  
 277 hydroxypropyl residues. In reality, the HP- $\gamma$ -CD structure is randomly substituted having  
 278 hydroxypropyl substituents at all positions of primary (C6 position) and secondary (C2 and  
 279 C3 position) interface. To simplify the molecular docking procedure, all hydroxyl groups ( $n =$   
 280 24) of the  $\gamma$ -CD molecule were substituted for the hydroxypropyl groups in the case of HP- $\gamma$ -  
 281 CD model. Alternatively, the theoretical binding ratio (BR) was simply defined as the  $\Delta G_{bind}$   
 282 ratio between the binding affinities of the CUR/ $\gamma$ -CD and CUR/HP- $\gamma$ -CD complexes as:

$$BR = \frac{\Delta G_{CUR/HP\text{-}\gamma\text{-CD}}}{\Delta G_{CUR/\gamma\text{-CD}}} \quad (5)$$

283 As shown in Figures 3 and 4, the CUR position is roughly detected to be docked in the center  
 284 of the CD structures using 1:1 complex stoichiometry, where the binding cavity is located.

285 This stoichiometry was confirmed via a good correlation between the experimental data and  
286 the 1:1 binding isotherm for the CUR/CD complexes (Hegge et al., 2009). However, the  
287 formation of inclusion complexes with 1:2 (guest:host) stoichiometry is possible for  
288 CUR/HP- $\gamma$ -CD as it was observed in the CUR absorption spectra using UV-Vis spectroscopy  
289 (Hegge et al., 2009). The theoretical molecular docking results were in good agreement with  
290 the experimentally derived data judging by the theoretical binding ratio for the standard (BR =  
291 1.15) and hydrated (BR = 1.29) molecular docking in comparison with the reference (BR<sub>ref</sub> =  
292 1.37).

293 Furthermore, the three monomers (CUR,  $\gamma$ -CD and HP- $\gamma$ -CD) and four inclusion complexes,  
294 including those with the hydrated ligand were minimized using the conjugate gradient  
295 approach in order to perform the single-point AM1 calculation on the assessment of their  
296 relative chemical stability. The AM1 energies of 7 species and the energy difference ( $\Delta E$ )  
297 between the inclusion complexes and their constituent monomers are reported in Table 3. The  
298 relative stabilities of CUR/CDs inclusion complexes were measured by evaluating their  $\Delta E$ ,  
299 which can be addressed as the stabilizing energy of complexation. Hence, the low  $\Delta E$  values,  
300 the more stable the inclusion complex. The energies of all the complexes were lower than the  
301 energies of their two constituents except for CUR/HP- $\gamma$ -CD, indicating that the association of  
302 CUR and CDs had formed mainly quite stable complexes. Among the four inclusion  
303 complexes, the more hydrated CUR/ $\gamma$ -CD complex was found with the lowest energy term  
304 ( $\Delta E = -191.55 \text{ kcal}\cdot\text{mol}^{-1}$ ) due to the numerous stabilizing CD intramolecular H-bonds and  
305 less excessive water displacement effect.

306 Additionally, in order to study the effect of the CDs on the CUR conformational change that  
307 can be adapted into the cavity, as well as their influence on the binding property, the CUR/CD  
308 complexes were subjected to the MC simulations implemented in the ROSETTA code (Meiler  
309 et al., 2006), and 100 ns MD simulations with the MM-GBSA approach in evaluating binding  
310 affinity. In classical MD simulations, the conformational changes of compounds and proteins  
311 are connected in time. These simulations mimic the dynamical behavior of the studied  
312 systems, from which time-dependent values of conformational and thermodynamic properties  
313 can be estimated. Series of atomic coordinates (trajectories) are output in the result by using  
314 Newton's equations of motion. However, in MC simulations, each conformation can be  
315 determined only on its predecessor. The MC protocol predicts conformations randomly and  
316 employs energetic criteria to detect whether or not to confirm the new conformation.

317 To approximate the MD simulations in a more or less realistic way, all the hydroxyl groups  
318 were substituted with hydroxypropyl residues in the case of modified cyclodextrin models.  
319 Since the biophysical and biological behaviors of a compound often depend mainly upon the  
320 conformations that it can adopt, the time-dependent configurations (translations and rotations)  
321 of the CUR into the  $\gamma$ -CD and HP- $\gamma$ -CD were studied and clearly monitored (Supplementary  
322 material 1 and 2) based on the MD trajectory frames, in which the CD heavy atoms were  
323 aligned with respect to the starting structure. These analyses are feasible to illustrate the level  
324 of the conformational changes and movements of the CUR into the different environments  
325 from the starting point. The efficiency of this fashion can be enhanced by clustering the  
326 different configurations of the CUR that group together the similar conformations, from  
327 which the representative conformers can be selected. The relatively straightforward clustering  
328 method is the RMSD parameter between pairs of conformations (sometimes referred to as  
329 distance analysis). The CUR spatial arrangements were set establishing non-bonded forces  
330 with the CDs atoms and the water molecules into the cavity. The strong binding of CUR into  
331 the HP- $\gamma$ -CD provides a high level of shape complementary with the hydrophobic pocket of  
332 the HP- $\gamma$ -CD.

333 The relative structural stability of the CUR in the HP- $\gamma$ -CD cavity is dependent upon internal  
334 and non-covalent forces between the modified CD and CUR atoms. The CUR molecule in the  
335 HP- $\gamma$ -CD complex incurs a higher entropic penalty compared to CUR in the  $\gamma$ -CD complex.  
336 The free energy difference is considered to be a highly important factor in the thermodynamic  
337 concept and it would appear to be necessary for estimating the average  $\Delta G_{\text{bind}}$  values between  
338 the CUR and CDs based on the MC and MD trajectory frames. The energetic analysis reveals  
339 that the highest CD binding affinity to CUR belongs to HP- $\gamma$ -CD after ligand hydration with  
340 the  $\Delta G_{\text{MM-GBSA}}$  value of  $-86.38 \text{ kcal}\cdot\text{mol}^{-1}$  and the  $\Delta G_{\text{bind}}$  value of  $-71.4 \text{ kcal}\cdot\text{mol}^{-1}$ . This was  
341 due to strong hydrophobic (vdW) forces causing a decrease in the CUR hydration followed by  
342 excessive desolvation effects increasing water displacement (Figure 5 and 6 [A-D]). On the  
343 other hand, the hydration/desolvation effect of CUR/ $\gamma$ -CD characterized by less water  
344 displacement and high ligand hydration was more pronounced. However, the hydrophobic  
345 (vdW) forces in CUR/ $\gamma$ -CD were less prominent.

346 Furthermore, the relative free energies of binding CUR to the hydrated and dehydrated CDs  
347 by the MD simulations were estimated to be  $-69.67 \text{ kcal}\cdot\text{mol}^{-1}$  and  $-46.44 \text{ kcal}\cdot\text{mol}^{-1}$ ,  
348 respectively. The same systems (CUR bound to hydrated/dehydrated  $\gamma$ -CD and HP- $\gamma$ -CD)  
349 were examined by the MC simulations, providing free energy differences of  $-51.90 \text{ kcal}\cdot\text{mol}^{-1}$

350 <sup>1</sup> and  $-49.41 \text{ kcal}\cdot\text{mol}^{-1}$ , respectively. Both simulation methods were able to accurately  
351 determine the effects of the combinatorial explicit and implicit solvent models of the cavity  
352 that were being used in the energy calculations. The stability of the CUR was a consequence  
353 of the hydrophobic effect in the pocket of the CDs, from which the contribution of the  
354 entropic term could be considered. The vdW forces between the CUR,  $\gamma$ -CD and HP- $\gamma$ -CD  
355 systems were calculated to be  $-27.59 \text{ kcal}\cdot\text{mol}^{-1}$  and  $-40.57 \text{ kcal}\cdot\text{mol}^{-1}$ , respectively. The  
356 vdW interactions of CUR/  $\gamma$ -CD and HP- $\gamma$ -CD in the presence of explicit water molecules  
357 showed the average energies to be  $-24.37 \text{ kcal}\cdot\text{mol}^{-1}$  and  $-37.03 \text{ kcal}\cdot\text{mol}^{-1}$ . The observed  
358 differences in the non-covalent energies for the explicitly hydrated and dehydrated pockets of  
359 the CDs were expected due to the water-mediated Coulombic forces. These results obtained  
360 through the MD simulations, obviously were in a satisfactory qualitative agreement with those  
361 calculated through the MC method. However, the relative free energy value was highly  
362 sensitive to the configurations of the CD complexes used for the above calculations. This was  
363 because, the conformations of the molecules were obtained by different simulation methods  
364 (MC and MD) in each case. This was considered to be a major drawback of the force-field  
365 methods. In principle, free energy is a very difficult value to estimate for flexible systems,  
366 such as the CDs used in the current study, which share many closely separated minima.  
367 Related thermodynamic terms, such as entropy and partial molar free energy, were also  
368 difficult to estimate, due to the poor sampling produced by these simulations.

369

#### 370 4. Conclusions

371 Molecular docking, MC, and MD simulations were performed in this study to investigate the  
372 CUR hydration/desolvation effects for its complexation with  $\gamma$ -CD and HP- $\gamma$ -CD. The  
373 calculations indicate that water molecules play an important role in host-guest complexation,  
374 mediating the binding of ligands with their targets via hydrogen bond formations. The CUR  
375 hydration increases its binding affinity to both CDs, which is confirmed by the  $\Delta G_{\text{bind}}$  and  
376  $\Delta G_{\text{MM-GBSA}}$  values. Although the CUR/CD complex affinities were significantly improved  
377 after the CUR hydration, as newly formed hydrogen bonds are responsible for the stability of  
378 the inclusion complexes, hydrophobic (vdW) forces in CUR/HP- $\gamma$ -CD are dominant over  
379 hydration/desolvation effects. In addition, the CUR/HP- $\gamma$ -CD complex was found to be more  
380 stable in aqueous solution with the highest apparent stability constant for CUR/HP- $\gamma$ -CD ( $K_c$   
381  $= 1.58 \cdot 10^4 \text{ M}^{-1}$ ) as the more soluble form in distilled water. Overall, the results of this study

382 can aid drug delivery vector development, underscoring the importance of hydration effect on  
383 the formulation of different drug-like molecules.

384

### 385 **Acknowledgments**

386 Special thanks are extended to Dr. Biswapriya B. Misra from the Department of Biology,  
387 Genetics Institute, University of Florida for his assistance in the paper's writing. The authors  
388 are also grateful to the BMBF (Bundesministerium für Bildung und Forschung) for supporting  
389 this work through a grant (BMBF13N11801) to Jens Broscheit.

390

### 391 **Conflicts of Interest**

392 The authors declare no conflict of interest.

393

### 394 **Reference**

- 395 1. Volate, S. R., D. M. Davenport, et al. (2005). "Modulation of aberrant crypt foci and  
396 apoptosis by dietary herbal supplements (quercetin, curcumin, silymarin, ginseng and  
397 rutin)." Carcinogenesis **26**(8): 1450-1456.
- 398 2. Baumann, L., H. Woolery-Lloyd, et al. (2009). "'Natural' ingredients in cosmetic  
399 dermatology." J Drugs Dermatol **8**(6 Suppl): s5-9.
- 400 3. Nagabhushan, M. and S. V. Bhide (1992). "Curcumin as an inhibitor of cancer." J Am  
401 Coll Nutr **11**(2): 192-198.
- 402 4. Prasad, S. and A. K. Tyagi (2015). "Curcumin and its analogues: a potential natural  
403 compound against HIV infection and AIDS." Food Funct **6**(11): 3412-3419.
- 404 5. Tonnesen, H. H., M. Masson, et al. (2002). "Studies of curcumin and curcuminoids.  
405 XXVII. Cyclodextrin complexation: solubility, chemical and photochemical stability."  
406 Int J Pharm **244**(1-2): 127-135.
- 407 6. Yadav, V. R., S. Suresh, et al. (2009). "Effect of cyclodextrin complexation of curcumin  
408 on its solubility and antiangiogenic and anti-inflammatory activity in rat colitis model."  
409 AAPS PharmSciTech **10**(3): 752-762.
- 410 7. Marcolino, V. A., G. M. Zanin, et al. (2011). "Interaction of curcumin and bixin with  
411 beta-cyclodextrin: complexation methods, stability, and applications in food." J Agric  
412 Food Chem **59**(7): 3348-3357.

- 413 8. Zidovetzki, R. and I. Levitan (2007). "Use of cyclodextrins to manipulate plasma  
414 membrane cholesterol content: evidence, misconceptions and control strategies."  
415 Biochim Biophys Acta **1768**(6): 1311-1324.
- 416 9. Baldwin, R. L. (2010). "Desolvation penalty for burying hydrogen-bonded peptide  
417 groups in protein folding." J Phys Chem B **114**(49): 16223-16227.
- 418 10. Forli, S. and A. J. Olson (2012). "A force field with discrete displaceable waters and  
419 desolvation entropy for hydrated ligand docking." J Med Chem **55**(2): 623-638.
- 420 11. Higuchi T, Connors KA. Phase solubility techniques. In: Reilly CN, editor. Advances in  
421 Analytical Chemistry Instrumentation. Vol. 4. New York, NY: Interscience; 1965. pp.  
422 117–212.
- 423 12. Pinotsis, N., D. D. Leonidas, et al. (2003). "The binding of beta- and gamma-  
424 cyclodextrins to glycogen phosphorylase b: kinetic and crystallographic studies."  
425 Protein Sci **12**(9): 1914-1924.
- 426 13. Bacheega, J. F., L. F. Timmers, et al. (2013). "GTKDynamo: a PyMOL plug-in for  
427 QC/MM hybrid potential simulations." J Comput Chem **34**(25): 2190-2196.
- 428 14. Gasteiger, J. and M. Marsili (1980). "Iterative Partial Equalization of Orbital  
429 Electronegativity - a Rapid Access to Atomic Charges." Tetrahedron **36**(22): 3219-  
430 3228.
- 431 15. Goodsell, D. S., G. M. Morris, et al. (1996). "Automated docking of flexible ligands:  
432 applications of AutoDock." J Mol Recognit **9**(1): 1-5.
- 433 16. Forli, S. (2015). "Charting a Path to Success in Virtual Screening." Molecules **20**(10):  
434 18732-18758.
- 435 17. Seeliger, D. and B. L. de Groot (2010). "Ligand docking and binding site analysis with  
436 PyMOL and Autodock/Vina." J Comput Aided Mol Des **24**(5): 417-422.
- 437 18. Dewar, M. J. S., E. G. Zoebisch, et al. (1985). "The Development and Use of Quantum-  
438 Mechanical Molecular-Models .76. Am1 - a New General-Purpose Quantum-  
439 Mechanical Molecular-Model." J Am Chem Soc **107**(13): 3902-3909.
- 440 19. Rocha, G. B., R. O. Freire, et al. (2006). "RM1: A reparameterization of AM1 for H, C,  
441 N, O, P, S, F, Cl, Br, and I." Journal of Computational Chemistry **27**(10): 1101-1111.
- 442 20. Bowers, K. J., R. O. Dror, et al. (2006). "The midpoint method for parallelization of  
443 particle simulations." Journal of Chemical Physics **124**(18).
- 444 21. Banks, J. L., H. S. Beard, et al. (2005). "Integrated modeling program, applied chemical  
445 theory (IMPACT)." J Comput Chem **26**(16): 1752-1780.

- 446 22. Essmann, U., L. Perera, et al. (1995). "A Smooth Particle Mesh Ewald Method." Journal  
447 of Chemical Physics **103**(19): 8577-8593.
- 448 23. Hoover, W. G. (1985). "Canonical Dynamics - Equilibrium Phase-Space Distributions."  
449 Physical Review A **31**(3): 1695-1697.
- 450 24. Martyna, G. J., D. J. Tobias, et al. (1994). "Constant-Pressure Molecular-Dynamics  
451 Algorithms." Journal of Chemical Physics **101**(5): 4177-4189.
- 452 25. Meiler, J. and D. Baker (2006). "ROSETTALIGAND: protein-small molecule docking  
453 with full side-chain flexibility." Proteins **65**(3): 538-548.
- 454 26. Gohlke, H. and D. A. Case (2004). "Converging free energy estimates: MM-PB(GB)SA  
455 studies on the protein-protein complex Ras-Raf." J Comput Chem **25**(2): 238-250.
- 456 27. Li, J., R. Abel, et al. (2011). "The VSGB 2.0 model: a next generation energy model for  
457 high resolution protein structure modeling." Proteins **79**(10): 2794-2812.
- 458 28. Ansari, M. Y.; Dikhit, M. R.; Sahoo, G. C.; Das, P., Comparative modeling of HGPRT  
459 enzyme of *L. donovani* and binding affinities of different analogs of GMP.  
460 *International journal of biological macromolecules* **2012**, 50 (3), 637-49.
- 461 29. Kar, R. K.; Ansari, M. Y.; Suryadevara, P.; Sahoo, B. R.; Sahoo, G. C.; Dikhit, M. R.;  
462 Das, P., Computational elucidation of structural basis for ligand binding with  
463 *Leishmania donovani* adenosine kinase. *BioMed research international* **2013**, 2013,  
464 609289.
- 465 30. Ahsan, M. J.; Choudhary, K.; Jadav, S. S.; Yasmin, S.; Ansari, M. Y.; Sreenivasulu, R.,  
466 Synthesis, antiproliferative activity, and molecular docking studies of curcumin  
467 analogues bearing pyrazole ring. *Med Chem Res* **2015**, 24 (12), 4166-4180.
- 468 31. Shityakov, S., R.E. Salmas, et al, (2016) "Characterization, In Vivo Evaluation and  
469 Molecular Modeling of Different Propofol-Cyclodextrin Complexes to Assess Their  
470 Drug Delivery Potential at The Blood-Brain Barrier Level" J Chem Inf Model **56**(10):  
471 1914-1922
- 472 32. Manolova, Y., V. Deneva, et al. (2014). "The effect of the water on the curcumin  
473 tautomerism: a quantitative approach." Spectrochim Acta A Mol Biomol Spectrosc **132**:  
474 815-820.
- 475 33. Tabushi, I., Y. I. Kiyosuke, et al. (1978). "Approach to Aspects of Driving Force of  
476 Inclusion by Alpha-Cyclodextrin." J Am Chem Soc **100**(3): 916-919.
- 477 34. Tanhuanpaa, K., K. H. Cheng, et al. (2001). "Characteristics of pyrene  
478 phospholipid/gamma-cyclodextrin complex." Biophysical Journal **81**(3): 1501-1510.

- 479 35. Munro, I. C., P. M. Newberne, et al. (2004). "Safety assessment of gamma-  
480 cyclodextrin." Regul Toxicol Pharmacol **39 Suppl 1**: S3-13.
- 481 36. Szejtli, J. (1998). "Introduction and General Overview of Cyclodextrin Chemistry."  
482 Chemical Reviews **98**(5): 1743-1754.
- 483 37. Uekama, K., F. Hirayama, et al. (1998). "Cyclodextrin Drug Carrier Systems."  
484 Chemical Reviews **98**(5): 2045-2076.
- 485 38. Ma, X. Y., Z. X. Liao, et al. (2000). "Study of the podophyllotoxin/beta-cyclodextrin  
486 inclusion complex." Journal of Inclusion Phenomena and Macrocyclic Chemistry **36**(3):  
487 335-342.
- 488 39. Zhao, D. Y., K. J. Liao, et al. (2002). "Study of the supramolecular inclusion of beta-  
489 cyclodextrin with andrographolide." Journal of Inclusion Phenomena and Macrocyclic  
490 Chemistry **43**(3-4): 259-264.
- 491 40. Shityakov, S., J. Broscheit, et al. (2012). "alpha-Cyclodextrin dimer complexes of  
492 dopamine and levodopa derivatives to assess drug delivery to the central nervous  
493 system: ADME and molecular docking studies." Int J Nanomedicine **7**: 3211-3219.
- 494 41. Shityakov, S. and C. Forster (2014). "In silico structure-based screening of versatile P-  
495 glycoprotein inhibitors using polynomial empirical scoring functions." Adv Appl  
496 Bioinform Chem **7**: 1-9.
- 497 42. Pawar, Y. B., B. Munjal, et al. (2012). "Bioavailability of a lipidic formulation of  
498 curcumin in healthy human volunteers." Pharmaceutics **4**(4): 517-530.
- 499 43. Furuki, T., F. Hosokawa, et al. (1993). "Microscopic Medium Effects on a Chemical-  
500 Reaction - a Theoretical-Study of Decarboxylation Catalyzed by Cyclodextrins as an  
501 Enzyme Model." J Am Chem Soc **115**(7): 2903-2911.
- 502 44. Hegge, A. B., M. Masson, et al. (2009). "Investigation of curcumin-cyclodextrin  
503 inclusion complexation in aqueous solutions containing various alcoholic co-solvents  
504 and alginates using an UV-VIS titration method. Studies of curcumin and  
505 curcuminoides, XXXV." Pharmazie **64**(6): 382-389.

506

507

508

509

510

511  
512  
513  
514  
515  
516  
517  
518  
519  
520  
521  
522  
523  
524  
525  
526  
527  
528  
529  
530  
531  
532  
533  
534  
535  
536  
537  
538  
539  
540  
541  
542  
543

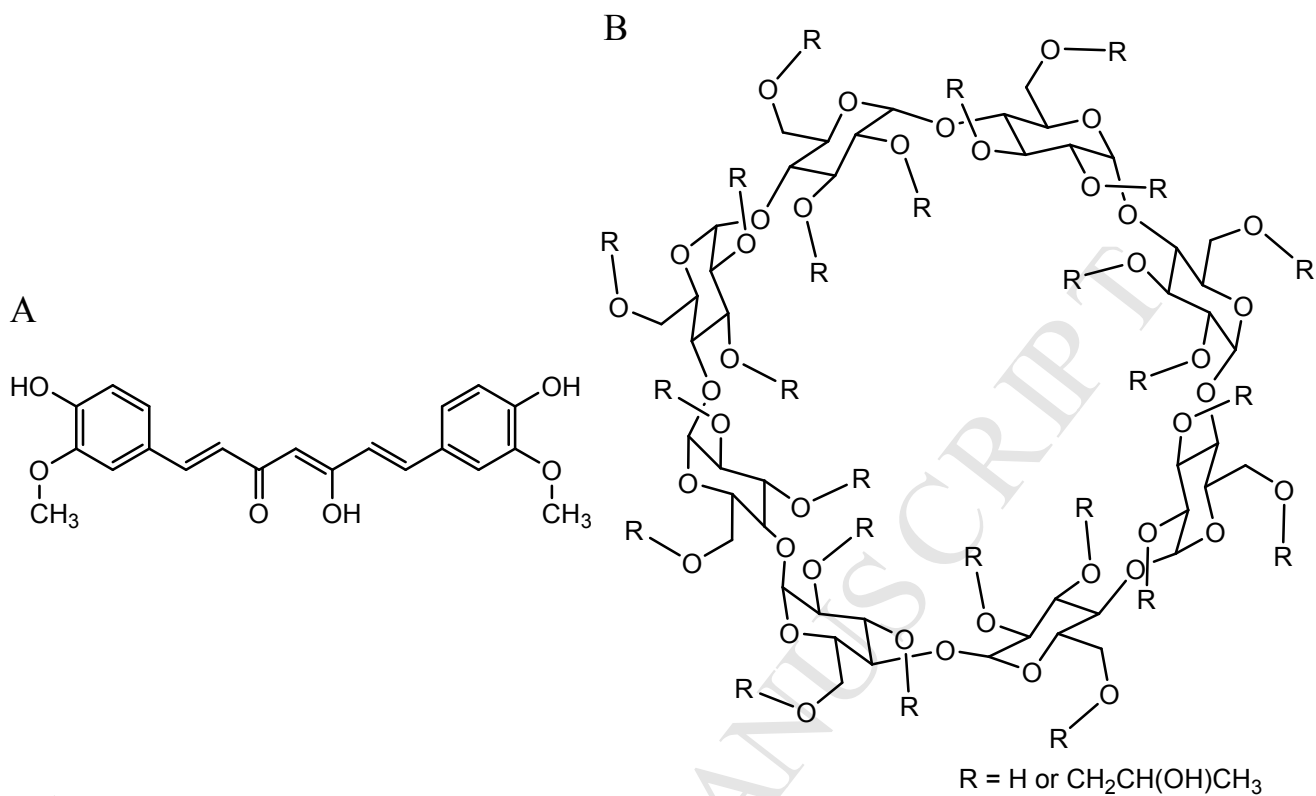
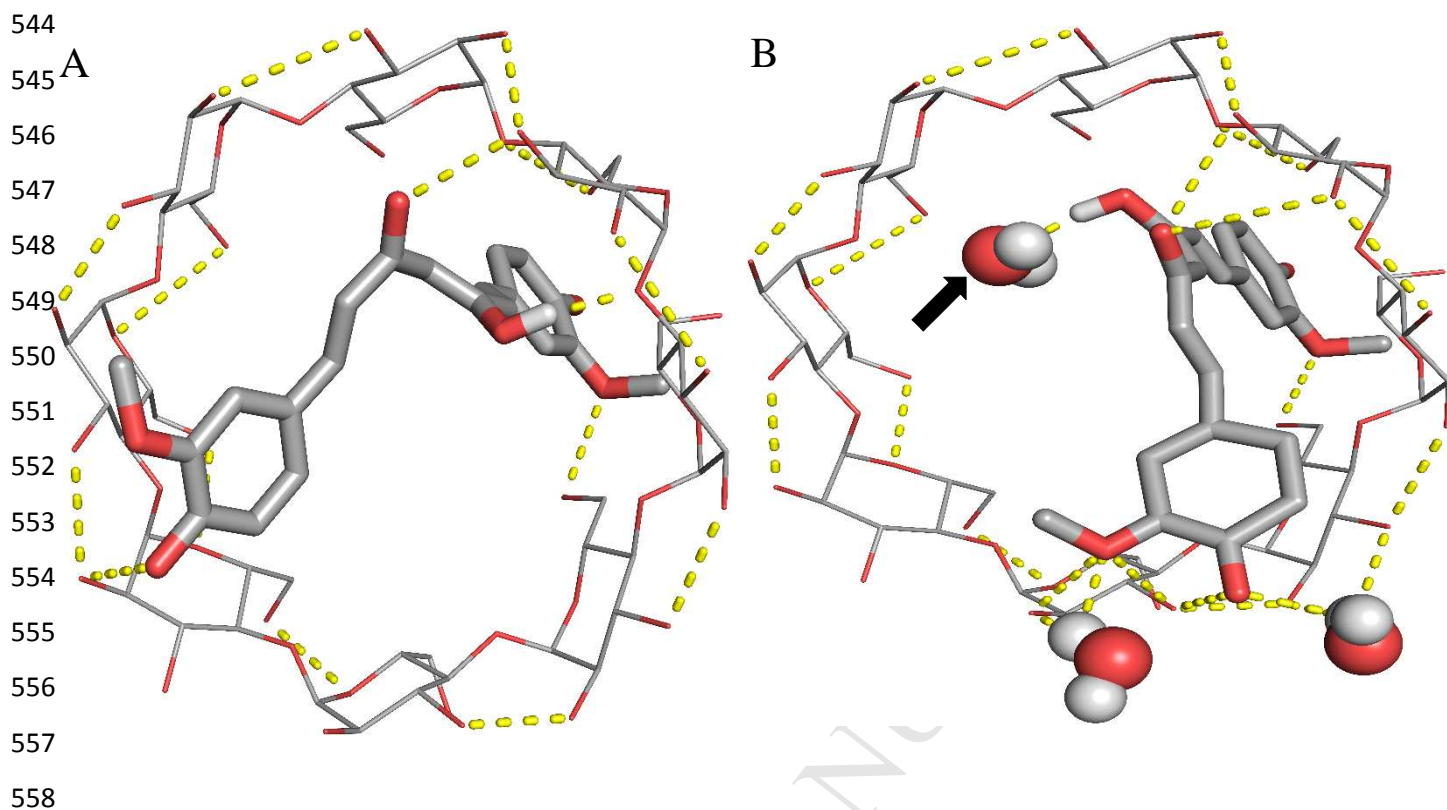


**Figure 1.** 2D chemical structure of CUR in enol form (A) and  $\gamma$ -CD (R = H) or HP- $\gamma$ -CD (R = CH<sub>2</sub>CH(OH)CH<sub>3</sub>) molecules (B)



559 **Figure 2:** Standard (A) and hydrated (B) AutoDock molecular docking profiles of CUR (enol  
560 form) bound to the  $\gamma$ -CD molecule. Cyclodextrin and its ligand are visualized with lines and  
561 sticks, respectively. Water molecules are represented in spheres, and the hydrogen bonds are  
562 depicted as yellow dashed lines. Water molecule located in the  $\gamma$ -CD binding cavity is pointed  
563 by the bold arrow. Molecules are colored according to their atom types. The majority of  
564 hydrogens atoms are omitted for clarity.

565  
566  
567  
568  
569  
570  
571  
572  
573  
574  
575  
576

577

578A

579

580

581

582

583

584

585

586

587

588

589

590

591

B

592 **Figure 3:** Standard (A) and hydrated (B) AutoDock molecular docking profiles of CUR (enol  
593 form) bound to the HP- $\gamma$ -CD molecule. Cyclodextrin and its ligand are visualized with lines  
594 and sticks, respectively. Water molecules are represented in spheres, and the hydrogen bonds  
595 are depicted as yellow dashed lines. Water molecule located in the  $\gamma$ -CD binding cavity is  
596 pointed by the bold arrow. Molecules are colored according to their atom types. The majority  
597 of hydrogens atoms are omitted for clarity.

598

599

600

601

602

603

604

605

606

607

608

609

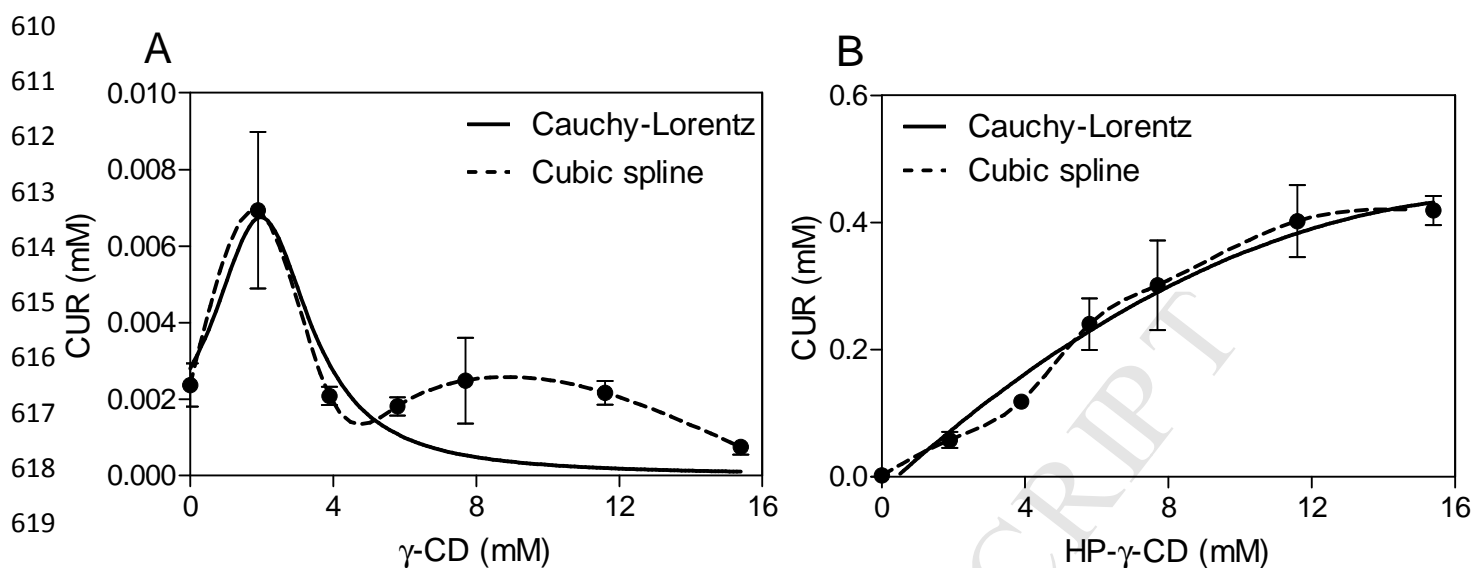


**Figure 4.** Solubility isotherms of the CUR/ $\gamma$ -CD (A) and CUR/HP- $\gamma$ -CD (B) complexes determined in H<sub>2</sub>O, pH 7.0. The  $S_0$  value (the same for both complexes) states for the CUR saturation concentration in the solvent in absence of cyclodextrin. The solid lines show fitting to the isotherms. The data represent means  $\pm$  S.D. of three independent experiments.

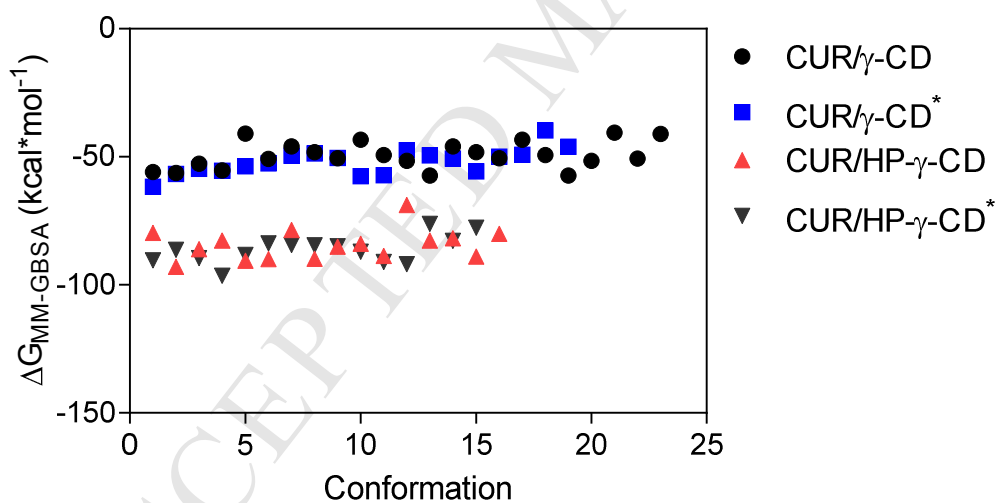
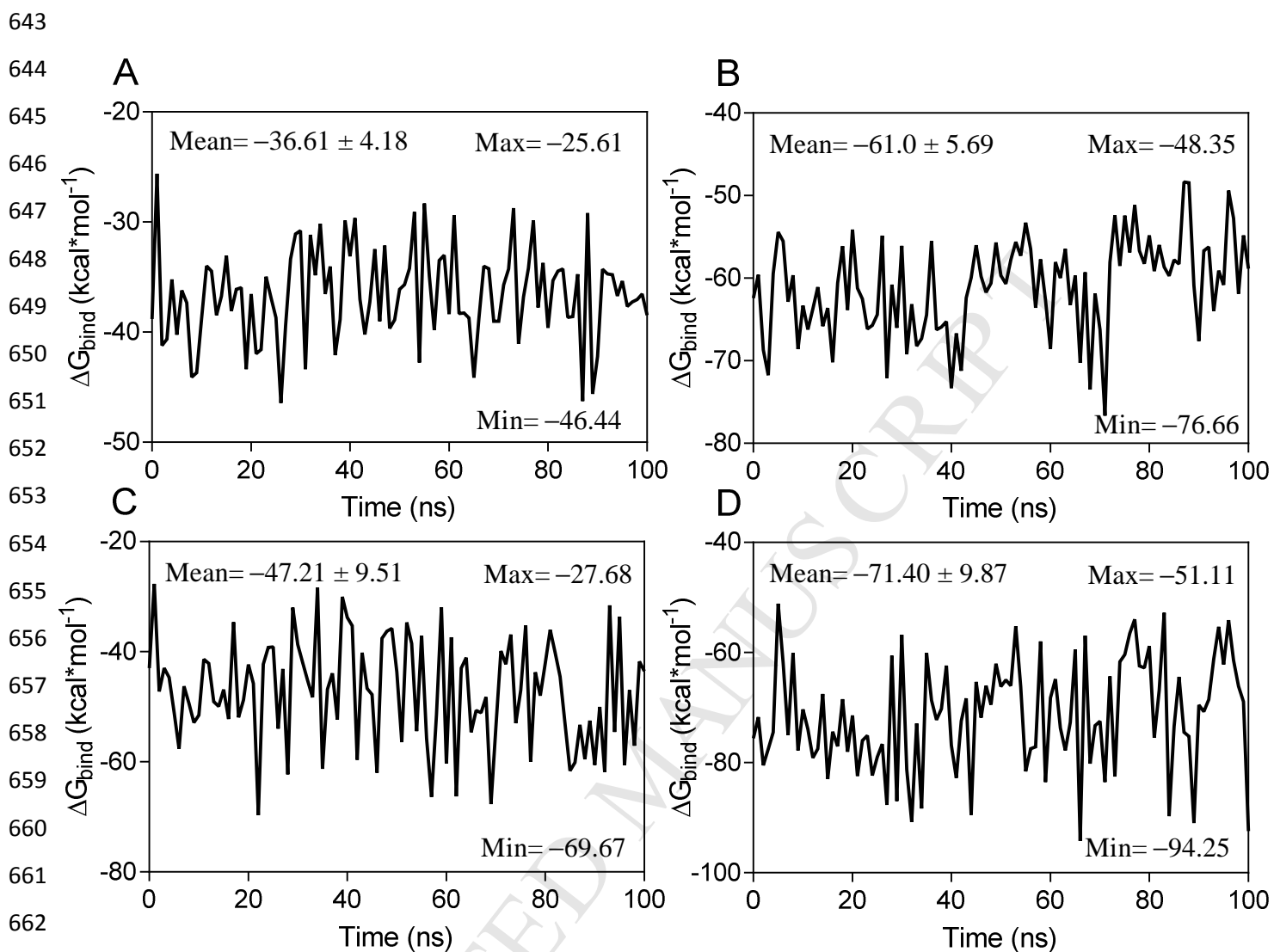


**Figure 5:** The  $\Delta G_{MM-GBSA}$  values for CUR/ $\gamma$ -CD and CUR/HP- $\gamma$ -CD with or without CUR hydration (denoted by \*) calculated by the MC approach.



664 **Figure 6:** The  $\Delta G_{\text{bind}}$  values (in  $\text{kcal}\cdot\text{mol}^{-1}$ ) calculated from 100 ns MD simulations for  
665 CUR/ $\gamma$ -CD and CUR/ $\gamma$ -CD\* (A, B) together with CUR/HP- $\gamma$ -CD and CUR/HP- $\gamma$ -CD\* (C, D).  
666 CUR hydration is denoted by an asterisk sign. The data represent means  $\pm$  S.D.

667  
668  
669  
670  
671  
672  
673  
674

675 **Table 1:** Summary of the molecular docking profiles for CUR bound to the  $\gamma$ -CD and HP- $\gamma$ -  
676 CD molecules.

Complex	$N_{run}$	$N_{cl}$	$\Delta G_{bind}$ (kcal* $mol^{-1}$ )	$K_d$ ( $\mu M$ )	$LE^{**}$	$RMSD_{LC}$ (nm)	$N_{ats}^{***}$	$N_{tors}$
CUR/ $\gamma$ -CD	100	66	-6.83	9.45	-0.23	78.02	30	10
CUR/ $\gamma$ -CD*	100	72	-7.69 <sup>†</sup>	2.2	-0.17	78.18	45	10
CUR/HP- $\gamma$ -CD	100	51	-7.92	1.49	-0.26	77.64	30	10
CUR/HP- $\gamma$ -CD*	100	65	-9.93 <sup>†</sup>	0.05	-0.22	77.25	45	10

677 \* -hydrated ligand; \*\* -  $LE = \frac{\Delta G_{bind}}{N_{ats}}$ ; \*\*\* -waters are described by monatomic pseudoatoms; <sup>†</sup> -

678  $\Delta G_{bind} = \Delta G_{lig} + \Delta G_{wat}$ ;  $N_{runs}$ -total number of runs;  $N_{cl}$ -number of distinct clusters formed in  
679 the clustering;  $RMSD_{LC}$ -the root-mean-square-deviation difference between the lowest energy  
680 conformation (LC) in the largest cluster and the reference ligand conformation;  $N_{ats}$ -number  
681 of heavy atoms;  $N_{tors}$ -number of torsions

682

683 **Table 2:** Summary of displaced (DISP), weakly (WK) and strongly (STR) bound water  
684 molecules during hydrated complexation of CUR with the  $\gamma$ -CD and HP- $\gamma$ -CD molecules.

Complex	DISP	WK	STR
CUR/ $\gamma$ -CD	12	2	1
CUR/HP- $\gamma$ -CD	13	1	1

685

686 **Table 3:** The AM1 energies (in kcal\* $mol^{-1}$ ) of the 7 species, the energy differences ( $\Delta E$ )  
687 between the inclusion complexes and the molecules (CUR,  $\gamma$ -CD and HP- $\gamma$ -CD), which form  
688 the complexes (CUR/  $\gamma$ -CD and CUR/HP- $\gamma$ -CD).

Species	AM1 energy	$\Delta E^{**}$
CUR	-151.19	-
$\gamma$ -CD	-1891.39	-
HP- $\gamma$ -CD	-3057.42	-
CUR/ $\gamma$ -CD	-2045.59	-3.01
CUR/ $\gamma$ -CD*	-2234.13	-191.55
CUR/HP- $\gamma$ -CD	-3199.91	8.7
CUR/HP- $\gamma$ -CD*	-3324.52	-115.91

689 \* -hydrated ligand; \*\* -  $\Delta E = E_{Complex} - E_{CD} - E_{CUR}$

- Curcumin solubility profiles and hydration/desolvation effects of this substance formulated with  $\gamma$ -cyclodextrin and hydroxypropyl- $\gamma$ -cyclodextrin were investigated.
- Curcumin/hydroxypropyl- $\gamma$ -cyclodextrin complex was found to be more stable in solution than curcumin/hydroxypropyl- $\gamma$ -cyclodextrin.
- Water molecules play an important role in host-guest complexation mediating the curcumin binding to cyclodextrins via hydrogen bond formations.
- Curcumin hydration/desolvation effects contributed to the complex formation by elevating the curcumin binding affinity to cyclodextrins.
- Curcumin/hydroxypropyl- $\gamma$ -cyclodextrin complex was determined with a minimal free energy of binding due to hydrophobic forces.